Analysis of X-Ray Spectra Obtained in Foam Z-Pinch Experiments

J.J. MacFarlane, P. Wang, T.J. Nash,
M.S. Derzon, G.A. Allshouse, C. Deeney

May 1996

UWFDM-1011

Presented at the 11th Topical Conference on High-Temperature Plasma Diagnostics, Monterey, CA, 12–16 May 1996; to be published in *Review of Scientific Instruments*.

FUSION TECHNOLOGY INSTITUTE

UNIVERSITY OF WISCONSIN

MADISON WISCONSIN

Analysis of X-ray Spectra Obtained in Foam Z-pinch Experiments

J. J. MacFarlane and P. Wang

Fusion Technology Institute
Department of Nuclear Engineering and Engineering Physics
University of Wisconsin-Madison
Madison, WI 53706

T. J. Nash, M. S. Derzon, G. A. Allshouse, and C. Deeney

Sandia National Laboratories
Albuquerque, NM, 87185

May 1996

UWFDM-1011

Presented at the 11th Topical Conference on High-Temperature Plasma Diagnostics, Monterey, CA, 12–16 May 1996; to be published in *Review of Scientific Instruments*.

Abstract

Foam Z-pinch experiments have recently been performed on SATURN to study issues associated with the initiation, acceleration, and stagnation phases of the pinch. Time-integrated x-ray crystal spectra have been recorded from experiments with 5 mg/cc Si aerogel loads and 10 mg/cc agar loads. In this paper, we describe results from collisional-radiative equilibrium calculations performed to analyze the Si, Na, and S K-shell emission observed in the spectra. Particular attention is paid to density and opacity effects on intensity ratios involving He_α, He intercombination, and Li-like satellite lines.

1. Introduction

Foam Z-pinch experiments have recently been performed on the SATURN pulsed-power device at Sandia National Laboratories.[1,2] In these experiments, SATURN drives low-density Si aerogel (SiO_2) and agar ($C_7H_{13}NO_5$) foam loads with currents of about 7 MA with a rise time of approximately 50 ns. The purpose of the experiments is to study the initiation, acceleration, and stagnation phases of the pinch. X-ray and EUV spectra were recorded using a crystal spectrometer and a Hettrick EUV spectrograph.[2] X-ray diode (XRD) array measurements and X-ray pinhole images were also recorded[1] with lines-of-sight along the pinch axis and at an angle of 35° with respect to the cylinder midplane.

In this paper, we discuss our analysis of time-integrated x-ray spectra obtained from 5 mg/cc Si aerogel and 10 mg/cc agar foam loads with 10 mm diameters. Figure 1 shows the spectra recorded from Shots 2249 (aerogel) and 2252 (agar). In the aerogel shot, Si K-shell lines from He- and H-like Si are clearly seen. In addition, satellites to the He_α and L_α can be observed. In the agar shot, K-shell lines from sodium and sulfur, which are impurities ($\sim 1\%$) in the agar, are observed. In both spectra, oxygen L_β, L_γ, and L_δ are observed at lower photon energies. However, because of the cutoff in the crystal spectra at about 0.7 keV, the oxygen L_α and He-like lines could not be recorded.

Below, we present results from collisional-radiative equilibrium (CRE) calculations for the aerogel and foam loads. The purpose of the calculations is to estimate the conditions of the relatively high-temperature x-ray emitting regions of the foam loads. To do this, we examine line intensity ratios of H-like to He-like lines and satellite-to-resonance lines of Si, Na, and S. This technique has been widely utilized in previous laboratory and astrophysical plasma studies.[3–6]

2. Models

Non-LTE atomic level populations and emergent spectra are computed using a collisional-radiative equilibrium model which solves multilevel statistical equilibrium equations self-consistently with the radiation field.[7,8] A total of 158 atomic levels were considered in the SiO_2 calculations (96 for Si, 62 for O), while a total of 239 levels were included in the agar calculations (38 for C, 7 for H, 43 for O, 77 for Na, and 74 for S). An L-S term-split energy level model was used. The selected levels were concentrated primarily around the Li-like ionization stage and higher. Autoionization states which contribute to the satellites of the He_α and L_α lines were also considered. These states are illustrated in the energy level diagram in Figure 2.

Processes considered in the calculations include collisional excitation, deexcitation, ionization and recombination; spontaneous decay; and autoionization and dielectronic recombination. In the aerogel results discussed below photoexcitation and photoionization were included. Here it was assumed that roughly 0.2% of the foam (by mass) contributed to the high-temperature x-ray emission. This assumption is based on the lack of a detectable bound-free continuum emission, which is predicted in simulations when larger x-ray emitting masses are assumed (e.g., $\gtrsim$ a few percent, depending on density). In the aerogel calculations, level populations were computed on a radial grid with cylindrical symmetry. A zone-to-zone escape probability model[9,10] was used to obtain emergent line intensities. This utilized Voigt line profiles which include the effects of natural, Doppler, Auger, and Stark broadening. In the agar calculations, the plasmas were assumed to be optically thin. This is justified because of the low Na and S concentrations in the agar.

Atomic cross section data were computed as follows. Energy levels, oscillator strengths, and autoionization rates were computed using a configuration interaction model with Hartree-Fock wavefunctions.[11] Collisional excitation rate coefficients for both allowed and forbidden transitions were computed using a distorted wave[12] model, while a Coulomb-Born[13] model was used to compute collisional ionization rate coefficients.

3. Results

CRE calculations were performed for Si aerogels and agar foams (with Na and S impurities) over densities ranging from 10^{19} to 10^{22} ions/cm^3 and temperatures ranging from 0.3 to 1.5 keV. The CRE results for line power densities were post-processed to examine various line ratio combinations for Na, S, and Si which included He- and H-like resonance lines and the satellites to the He_α and L_α lines. Below, after a brief discussion of this agar spectrum, we shall focus primarily on the Si aerogel simulations because of the better signal-to-noise ratio obtained in Shot 2249. In particular, we focus on the satellite and intercombination lines adjacent to the Si He_α line.

Estimates of the Na H-like to He-like line ratios measured in Shot 2252 suggest a temperature of approximately 0.4 - 0.6 keV. On the other hand, the S L_α to He_α line ratio is more consistent with a temperature of 1 keV. This apparent inconsistency results from the spectrometer viewing several relatively hot regions of the agar which have a broad range of plasma conditions. This is consistent with x-ray images,[1] which show substantial spatial variations in the x-ray emission.

Similar spatial variations are seen in the Si aerogel experiments, making it difficult to reproduce the entire Si K-shell spectrum with a single set of plasma temperature and density conditions. We therefore choose to focus our attention on the spectral region near the Si He_α line.

Figure 3 shows the ratio of the sum of the He intercombination (IC) line plus the Li-like *mn* and *st* satellites to the He_α line. We choose the sum of the former lines because they are not spectrally resolved in the crystal measurements. Results assuming a cylindrical mass of 6 μg/cm (or $\sim 0.2\%$ of the aerogel load by mass) are compared with optically thin intensity ratios on the bottom. As noted in earlier studies[4,5] resonant self-absorption of the He_α line can significantly affect the densities inferred from IC-to-resonance line ratios. Note that while the I(IC + *mn* + *st*)/I(He_α) ratio is relatively insensitive to temperature

in the optically thin case, it shows a pronounced dependence on temperature in the finite mass case for densities above 10^{20} ions/cm^3.

Figure 4 shows similar results for the ratio of the sum of the Li-like satellites [IC + $mn + st$] to the [$qr + abd + jk$] lines. Note that in this case, the finite mass results are very similar to the optically thin results for temperatures above approximately 0.6 keV. This occurs because the populations of the lower states of the Li-like satellite lines (i.e., the $1s^2\,2s\,{}^2$S and $1s^2\,2p\,{}^2$P states), and hence their optical depths, are small because He-like is the dominant ionization stage. Thus, this ratio shows a good density sensitivity, and remains relatively unaffected by opacity effects for the conditions shown.

In Figure 5 we compare the results of a calculated spectrum near the Si He$_\alpha$ line for the Si aerogel with the experimental spectrum for Shot 2249. The conditions assumed in the calculation are: $T = 400$ eV, $n = 3 \times 10^{19}$ ions/cm^3, and a mass of 6 μm/cm. The spectrum at the top is the calculated spectrum, where the Li-like satellites and He IC and He$_\alpha$ lines are clearly resolved. Assuming a spectral resolution of $\lambda/\Delta\lambda = 250$, the calculated spectrum, taking into account instrumental broadening, is represented by the dashed line with circles at the bottom. The solid curve is the experimental spectrum. Note that reasonably good agreement is achieved in this spectral region for these conditions. However, we note that a (second) higher temperature plasma region is required to account for the H-like Si line intensities seen by the spectrometer. Nevertheless, the calculations do suggest the x-ray-emitting region responsible for the observed structure in the He$_\alpha$ spectral region was probably at a relatively low density ($\sim 3 \times 10^{19}$ ions/cm^3; $n_e \sim 3 \times 10^{20}$ cm^{-3}). By comparison, the initial density of the SiO_2 load in this experiment was 5 mg/cc, or 1.5×10^{20} ions/cm^3. Thus, the plasma causing the He$_\alpha$ emission in this shot was likely not in a compressed state, but may have been at a somewhat lower density than its original state.

4. Summary

CRE calculations have been performed to analyze spectra obtained in initial foam Z-pinch experiments at SATURN. The SATURN x-ray spectra exhibit Si K-shell emission in Si aerogel experiments, and emission from the Na and S impurities in the agar foams. We have examined, in particular, density and opacity effects on the ratios of satellite-to-resonance and satellite-to-intercombination lines in the Si He_α spectral region. It is expected that x-ray spectroscopic diagnostic capabilities will be further enhanced in future SATURN and PBFA-Z experiments.

Acknowledgement

This work was supported in part by Sandia National Laboratories.

References

1. M. S. Derzon et al., these proceedings (1996).

2. T. J. Nash, M. S. Derzon, G. Allshouse, C. Deeney, D. Jobe, J. McGurn, J. J. MacFarlane, and P. Wang, these proceedings (1996).

3. C. DeMichelis and M. Mattioli, *Nuclear Fusion* **21**, 677 (1981).

4. D. Duston and J. Davis, *Phys. Rev. A* **21**, 1664 (1980).

5. J. P. Apruzese, D. Duston, and J. Davis, *J.Q.S.R.T.* **36**, 339 (1986).

6. R. Mewe, E. Gronenschild, and G. van den Oord, *Astron. Astrophys. Suppl. Ser.* **62**, 197 (1985).

7. J. J. MacFarlane, P. Wang, J. E. Bailey, T. A. Mehlhorn, R. J. Dukart, and R. F. Mancini, *Phys. Rev.* **E47**, 2748 (1993).

8. J. J. MacFarlane, "NLTERT – A Code for Computing the Radiative Properties of Non-LTE Plasma," University of Wisconsin Fusion Technology Institute Report UWFDM-931 (December 1993).

9. J. P. Apruzese, J. Davis, D. Duston, and K. G. Whitney, *J. Quant. Spectrosc. Radiat. Transfer* **23**, 479 (1980).

10. J. P. Apruzese, *J. Quant. Spectrosc. Radiat. Transfer* **34**, 447 (1985).

11. P. Wang, J. J. MacFarlane, and G. A. Moses, *Phys. Rev.* **E48**, 3934 (1993).

12. I. I. Sobelman, L. S. Vainshtein and E. A. Yukov, Excitation of Atoms and Broadening of Spectral Lines, Springer-Verlag, NY (1981).

13. A. Burgess, and M. C. Chidichimo, *Mon. Not. R. Astr.Soc.* **203**, 1269 (1982).

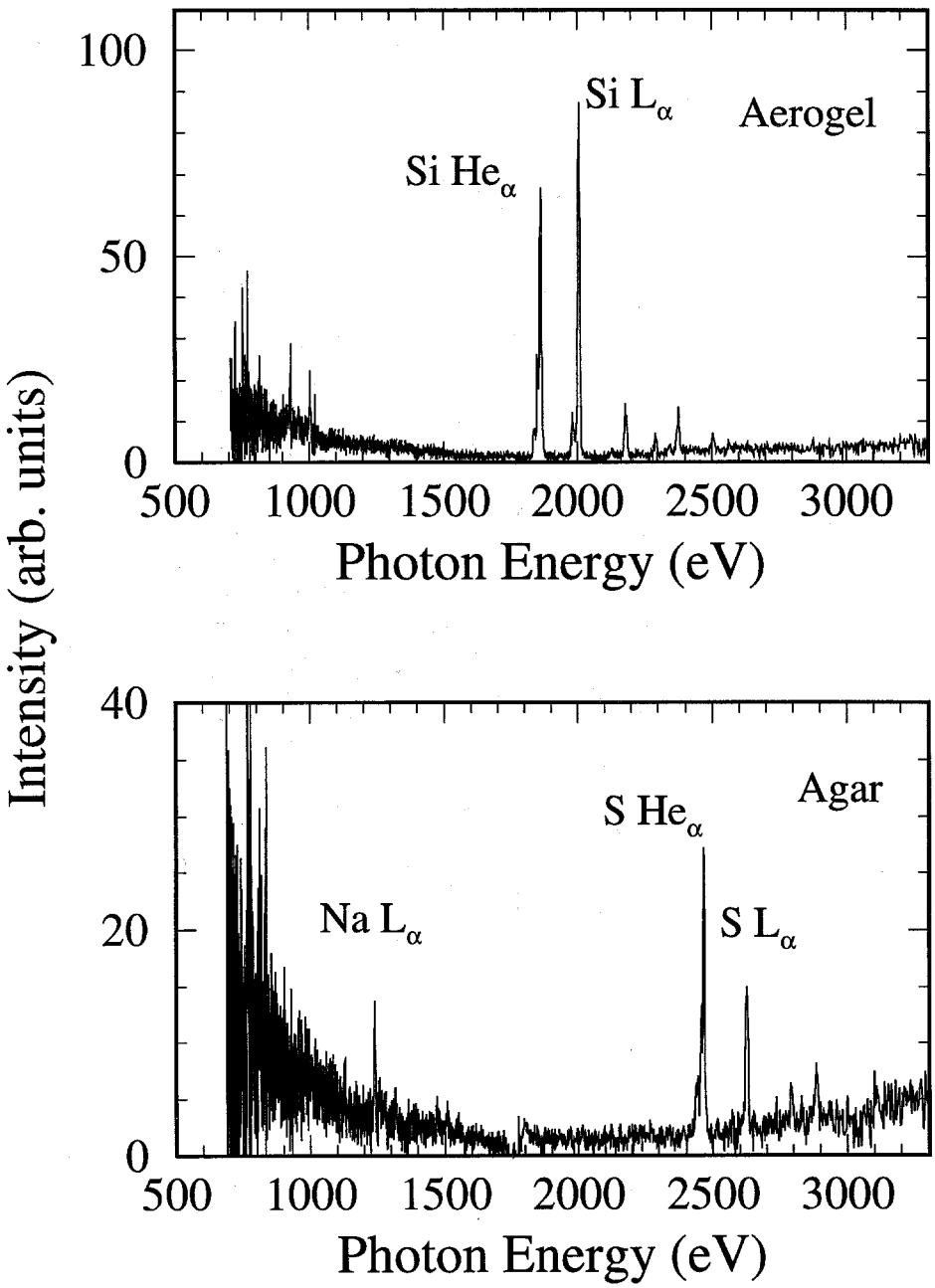

Figure 1. Time-integrated x-ray spectra for Shot 2249 (Si aerogel load) and Shot 2252 (agar load).

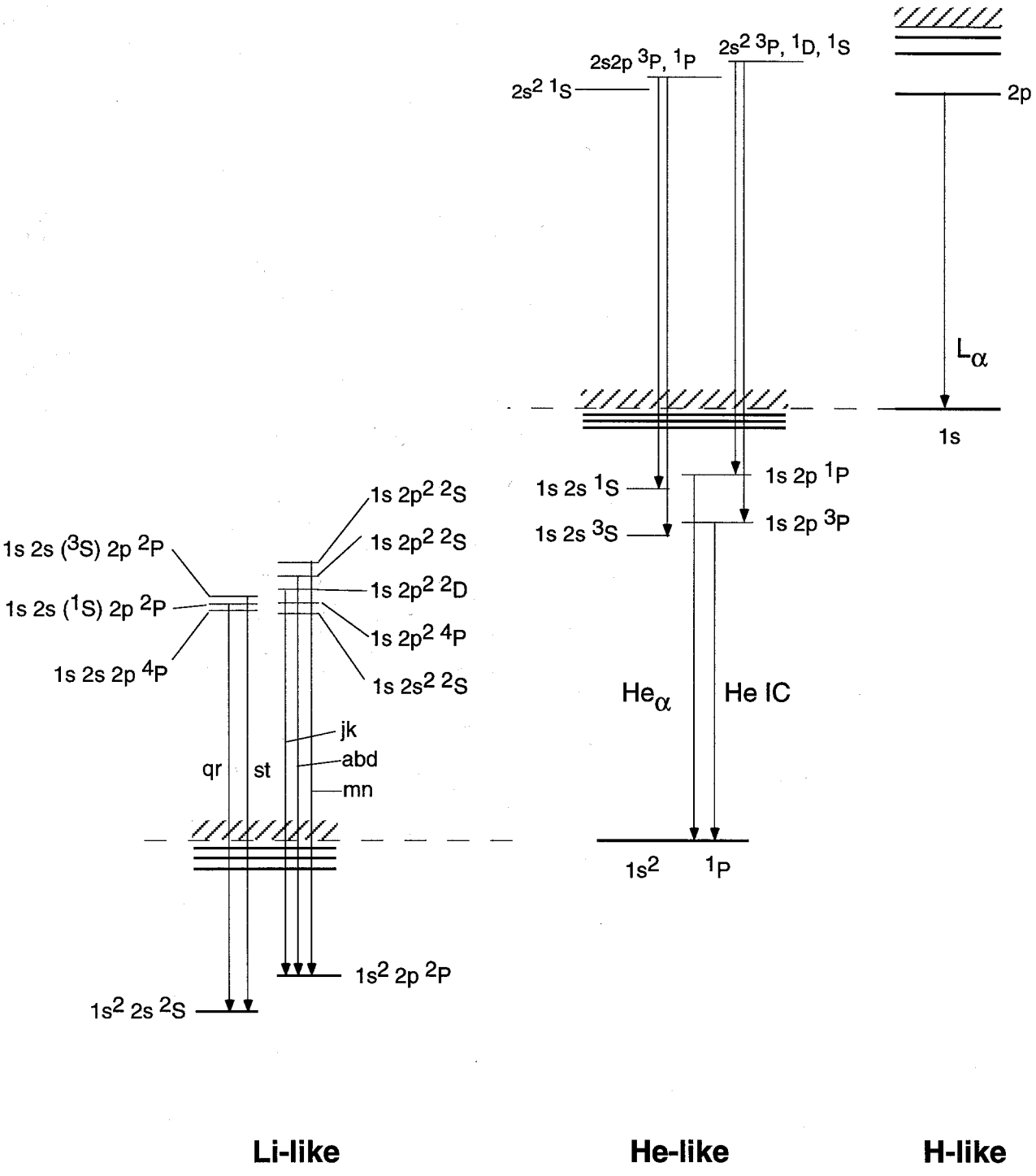

Figure 2. Schematic energy level diagram showing He_α and L_α lines and their satellites.

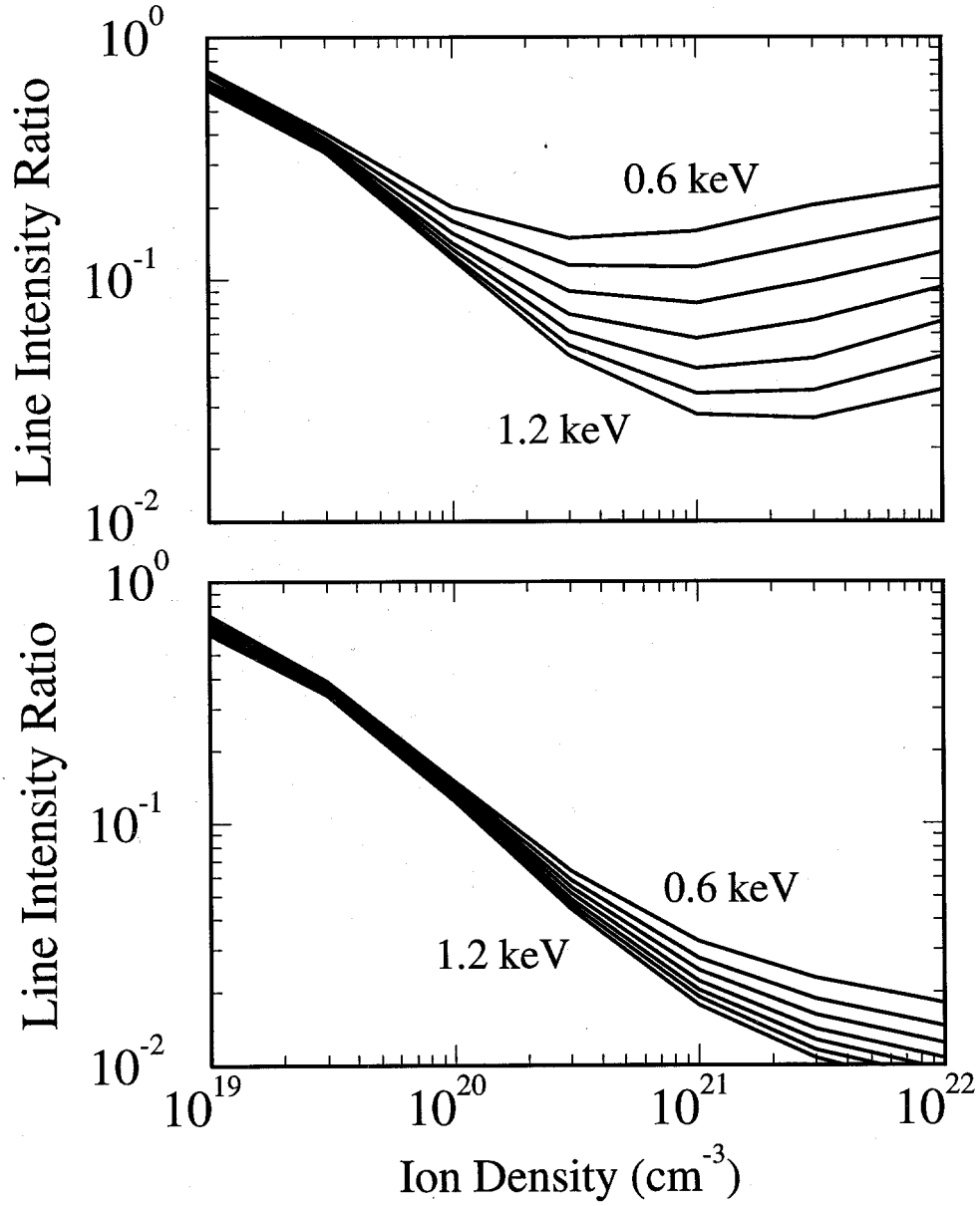

Figure 3. Intensity ratios for He IC plus Li-like satellites ($mn+st$) to the He_α line for SiO_2 plasmas. (Top) For a finite cylindrical mass of 6 μg/cm. (Bottom) Optically thin case. Curves correspond to temperatures ranging from 0.6 to 1.2 keV in increments of 0.1 keV.

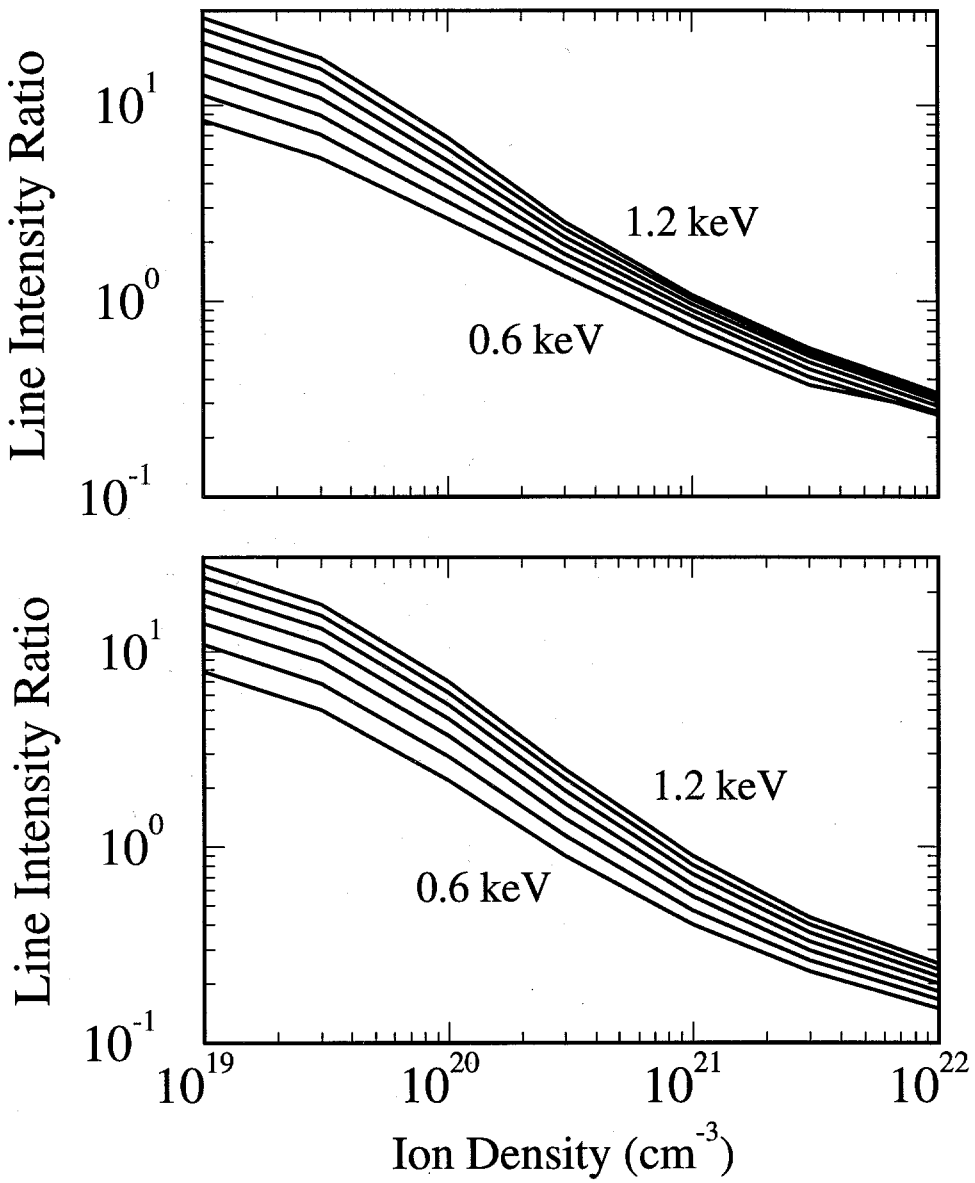

Figure 4. Intensity ratios for He IC plus Li-like satellites ($mn + st$) to Li-like satellites ($jk + qr + abd$) for SiO_2 plasmas. (Top) For a finite cylindrical mass of 6 μg/cm. (Bottom) Optically thin case. Curves correspond to temperatures ranging from 0.6 to 1.2 keV in increments of 0.1 keV.

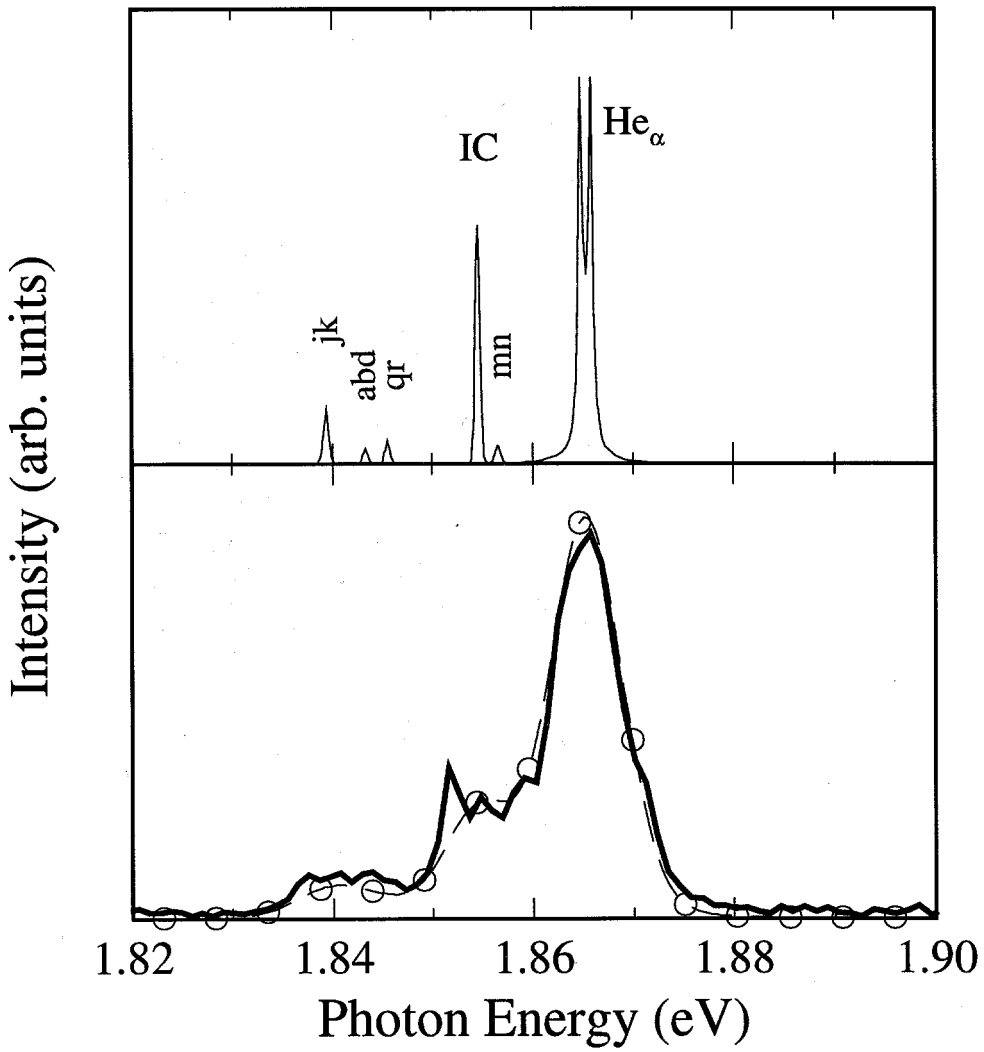

Figure 5. (Top) Calculated spectrum near Si He$_\alpha$ line for an SiO_2 plasma at $T = 400$ eV, $n = 3 \times 10^{19}$ ions/cm^3, and $M = 6\,\mu$g/cm. (Bottom) Comparison of calculated spectrum including instrumental response of $\lambda/\Delta\lambda = 250$ (dashed curve with circles) and experimental spectrum from Shot 2249 (solid curve).